THE ISOLATION OF MOUSE HEPATOCYTE GAP JUNCTIONS

Preliminary Chemical Characterization and X-Ray Diffraction

DANIEL A. GOODENOUGH and WALTHER STOECKENIUS

From the Cardiovascular Research Institute, University of California, San Francisco Medical Center, San Francisco, California 94122. Dr. Goodenough's present address is the Department of Anatomy, Harvard Medical School, Boston, Massachusetts 02115.

ABSTRACT

A method is reported for isolating a preparation of hepatic gap junctions from the mouse. The method involves a collagenase digestion, treatment with the detergent Sarkosyl NL-97, and ultrasonication, followed by sucrose gradient ultracentrifugation. A run with 36 animals yields 0.1–0.5 mg protein. Electron microscopy with thin-sectioning and negative staining techniques reveals that the final pellet is a very pure preparation of gap junctions, accompanied by a small amount of amorphous contamination. Polyacrylamide-gel electrophoresis of sodium dodecyl sulfate (SDS)-solubilized material shows one major protein in the junction, with an apparent mol wt of 20,000, and two minor components. Thin-layer chromatography demonstrates one major and one minor phospholipid, and some neutral lipid. Low-angle X-ray diffraction of wet and dried specimens show reflections which index on an 86 A center-to-center hexagonal lattice, corresponding closely to electron microscope data. Dried specimens also show a lamellar diffraction, corresponding to the total profile thickness of the junction (150 A).

INTRODUCTION

For a long time the erythrocyte ghost was the only cell membrane that was available in the quantity and purity necessary for correlated chemical and morphological studies. In recent years several new preparations of isolated cell membranes have been described. In general, cell membranes carry out many different functions which are localized in differentiated functional sites (37) The composition and structure of these functional sites can be expected to differ considerably from each other and from the rest of the membrane. Investigations of isolated whole cell membranes will yield data which represent an average of the many different functional sites and are therefore of limited value for an elucidation of the relation between structure and function It appears desirable to obtain preparations which contain one specific site in high concentration. We describe here the isolation of the gap junction which represents such a functional site or, more suitably described, a regular array of many identical sites: a specialized domain in the cell membrane.

The gap junction, or nexus, is a specialized area in the plasma membranes of two apposed cells It is recognized by its characteristic morphology. A polygonal lattice of globular substructures is visible in the junction after staining with lanthanum (15, 33), after freeze fracturing (6, 15, 23,

26), or after negative staining (2, 3, 15). Its characteristic appearance serves as a marker useful both during the isolation of the gap junctions and for determining the purity of the final preparations. The center-to-center subunit distance of the lattice has been estimated at 90 A (15, 33) and the over-all thickness of the junctions comprising the plasma membranes of both cells at 150 A (15, 34). Gap junctions have also been described in plasma membrane fractions of rat liver (3) and goldfish medulla (40, 41).

The gap junction is believed to be the site, in certain tissues, of intercellular passage of ions and larger molecules (1, 7, 11, 12, 13, 15–18, 22, 24, 26, 27, 30–32, 34). The coexistence of gap and septate junctions in a variety of invertebrates (9, 14, 19, 20, 28, 35) implicates the gap junction as the site of electrotonic coupling in these tissues as well Thus, the isolation of gap junctions with apparently unaltered morphology in sufficient quantity and purity for chemical studies, antibody production, and X-ray diffraction analysis can be expected to aid us substantially in an understanding of the molecular mechanisms involved in intercellular communication.

MATERIALS AND METHODS

Mature mice obtained from Simonson Breeding Laboratory (Gilroy, California) were used throughout

Fixation was performed as described previously (15). For freeze cleaving, small pieces of fixed liver were treated with 20% glycerol in 0 1 M cacodylate buffer for 1 hr. Freeze-cleaved replicas were then prepared using a Balzers apparatus (Balzer High Vacuum Corporation, Liechtenstein) at −115°C

Isolation of Junctions

Preparations of crude membranes were isolated as described previously (15). The final preparation of the gap junctions was isolated from this crude pellet.

After isolation on the discontinuous gradient, the crude pellet was collected and washed two times in 0.9% NaCl adjusted to pH 7.4 with saturated $NaHCO_3$ by sedimentation at 4000 rpm for 10 min in the Sorvall SS-34 rotor (Ivan Sorval, Inc., Norwalk, Conn.). The final pellet was resuspended in 10 ml of 0 1% collagenase and 0.1% hyaluronidase (type 1, Sigma Chemical Co., St Louis, Mo.) in bicarbonate-saline and digested for 1 hr at room temperature.

The membranes were then pelleted at 4000 rpm for 10 min in the Sorvall SS-34 rotor and resuspended in bicarbonate buffer (1 mM $NaHCO_3$, pH 8.2) at room temperature. To this suspension was added 10 ml of 1% Sarkosyl NL-97 (Geigy Chemical Corp., Ardsley, N. Y) to give a final concentration of 0.5% detergent The solution was then ultrasonicated for 6 sec at medium power with the probe inserted directly into the membrane-detergent solution (Sonic Dismembrator, Quigley Rochester, Rochester, N. Y.). Longer sonication reduced the junctions to successively smaller fragments.

After sonication, the preparation was allowed to stand for 10 min at room temperature and was then centrifuged for 15 min at 20,000 rpm in the Sorvall SS-34 rotor. The supernatant was discarded, and the residual pellet, now greatly reduced in size, was resuspended in 1 ml of bicarbonate buffer and layered at the top of a continuous linear sucrose gradient with $d = 1.20$ and $d = 1.127$ the limiting densities The gradients were spun at 283,000 g for 40 hr at 2°C.

The gradients were then collected in 12-drop samples along with dummy gradients used for measuring sucrose densities. Absorption of fractions was read at 280 mμ. The tubes containing the junctions were pooled and pelleted at 283,000 g for 1 hr. These final pellets were then used for electron microscopy, chemical analysis, and X-ray diffraction. Usually, 36 mouse livers were used per run.

Junctions were negatively stained on carbon-coated Formvar grids with sodium phosphotungstate at pH 7.0.

Thin-layer chromatography of chloroform-methanol extracts of junctions was done as described previously (15), using the solvent system of Wagner et al. (38).

Disk electrophoresis was done on 7.5% acrylamide gels (25) with 1% sodium dodecyl sulfate (SDS). Samples were solubilized in 1% SDS for 1 hr before electrophoresis at room temperature Gels were run at 2 ma per gel until bromphenol blue markers had run three-fourths the tube length The gels were then fixed overnight in 20% 5-sulfosalicylic acid, stained in 0.25% Coomassie blue in 50% methanol-acetic acid (10:1) for 4–6 hr, and destained in several changes of acetic acid-methanol-water (7.5:5:87.5) over a period of days. Photographs of the gels were scanned with a Joyce-Loebel scanning microdensitometer (Joyce, Loebel & Co., Inc., Burlington, Mass.).

X-ray diffraction was done with a Franks camera (10) using a doubly reflected beam of CuKα radiation from a Jarrell-Ash X-ray generator (Jarrell Ash Div , Fisher, Scientific Co , Waltham, Mass) passed through a nickel filter. Diffraction distances were varied between 7 and 10 cm and were calibrated using crystal of uranyl stearate Pellets of centrifuged junctions were introduced into 0.5 mm glass capillaries which were then heat-sealed. Dried specimens were allowed to dry at 4°C in the capillaries before sealing. X-ray photographs were taken with the camera evacuated to 1 mm Hg, exposures lasting from 24 to 48 hr.

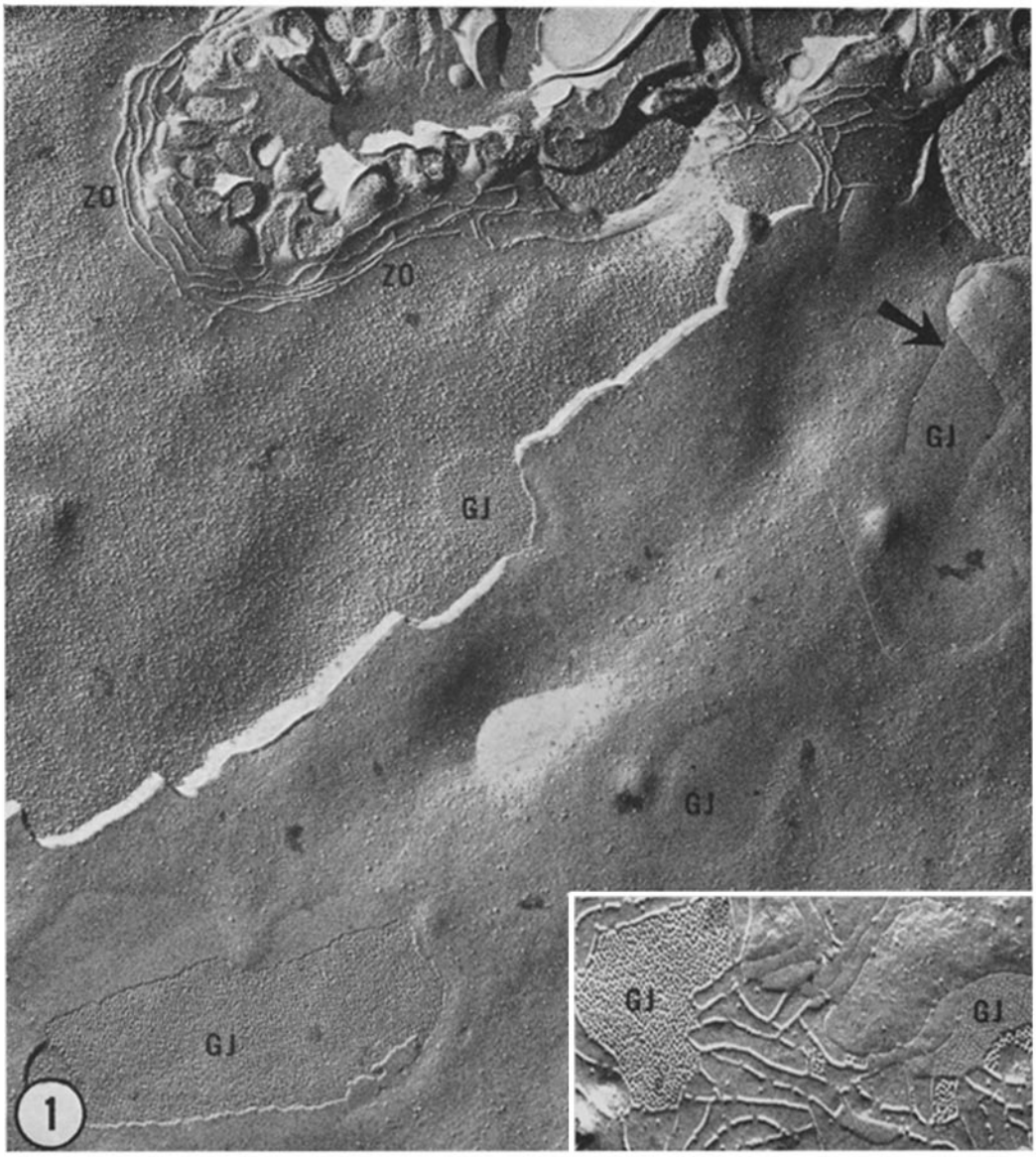

FIGURE 1 A freeze-fracture replica of whole mouse liver. A bile canaliculus is seen at the top of the figure closely surrounded by a weblike zonula occludens (*ZO*). At variable distances from the canaliculus, four gap junctions (*GJ*) may be seen. At the top right (arrow) a thread of zonula occludens has branched from the main body of the junction and partially encompasses a gap junction macula. The inset shows a portion of a freeze-fractured zonula occludens in mouse liver. In this area, gap junctions (*GJ*) are seen completely sequestered within the chambers between the ridges and furrows of the zonula occludens. × 41,100, Inset, × 65,700.

Films were scanned with a Joyce-Loebel scanning microdensitometer

RESULTS

The gap junction in whole mouse liver may assume a variety of macular shapes. As seen in Fig. 1, the gap junction is easily distinguished in freeze-cleaved material from areas of nonjunctional plasma membrane and from the weblike zonula occludens. Occasionally, tiny gap junctions are sequestered within the chambers between the threadlike contacts of the zonula occludens (23;

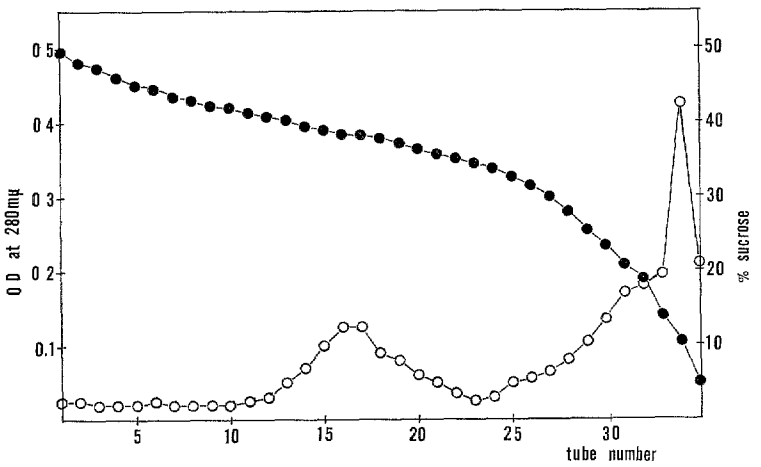

FIGURE 2 Optical density (*OD*), at 280 mμ, of the fractions collected from the continuous sucrose gradients (open circles). The closed circles show the concentration of sucrose in a parallel gradient collected in similar samples. Most of the sample stays at the top of the gradient (tubes 25–35). A small amount of material, the gap junctions, penetrates the gradiant and bands in tubes 14–20.

and inset, Fig. 1), and solitary threads of the zonula occludens may branch from the main body of the web structure and partially encompass a nearby gap junction plaque (arrow, Fig. 1) Although the two junctional types are occasionally intimately associated, the isolation procedure separates the zonulae occludentes and the nonjunctional plasma membranes from the gap junctions.

The continuous gradient concluding each run as described in the Methods section was collected in 12-drop samples On several runs, blank gradients were also collected in parallel and the sucrose densities of the samples were determined by refractometry (Fig 2) Most of the sample remained at the top of the gradient A small amount of material, the gap junctions, entered the gradient and banded at roughly 38% sucrose (d = 1.16) The amount of protein in this band is small (0 1–0 5 mg) and represents the yield from 36 animals. Micrographs of sections of the final isolated pellet are shown in Figs. 3 and 4 Fig. 3 demonstrates that the pellet contains mostly gap junctions of varying sizes, with very little contaminating material. Fig. 4 shows the isolated junctions at a higher magnification. The 2 nm gap characteristic of these junctions is intact (small arrows) At this higher magnification, an amorphous contamination in the preparation is evident (*AC* in Fig 4). This contamination appears in varying amounts from preparation to preparation Due to its association with the ends of the gap junctions (large arrow, Fig. 4), it is thought to be of nonjunctional plasma membrane origin.

Figs 5 and 6 are micrographs of negatively stained samples of isolated material. The polygonal lattice of subunits appears intact and there is very little nonjunctional material visible in the preparation.

The gap junctions are disrupted by 0 1–1 0% SDS Polyacrylamide gel electrophoresis with SDS of the solubilized junction preparation is shown in Fig. 7 *a*, tube 6 One major band is seen migrating between the pancreatic RNase (mol wt 13,000) and trypsin (mol wt 23,000) markers. There are also two minor bands, one of heavier and the other of lighter molecular weight It is not known if these minor components are junctional proteins or if they are related to the amorphous contamination seen in Fig 4

Fig 7 *b* is a microdensitometric scan of tube 6 The differences in intensity and hence relative concentration between the major peak and the two minor peaks may be seen Before a molecular weight can be determined from the electrophoresis data, these junctional proteins must be checked for carbohydrate moieties (36).

Fig. 8 shows a drawing of a thin-layer chromatogram of the lipids extracted from the isolated gap junction preparation There is only one major phospholipid, tentatively identified as phosphatidylcholine, and a minor component with an R_f similar to that of phosphatidylethanolamine In addition, there is some neutral lipid migrating at the solvent front

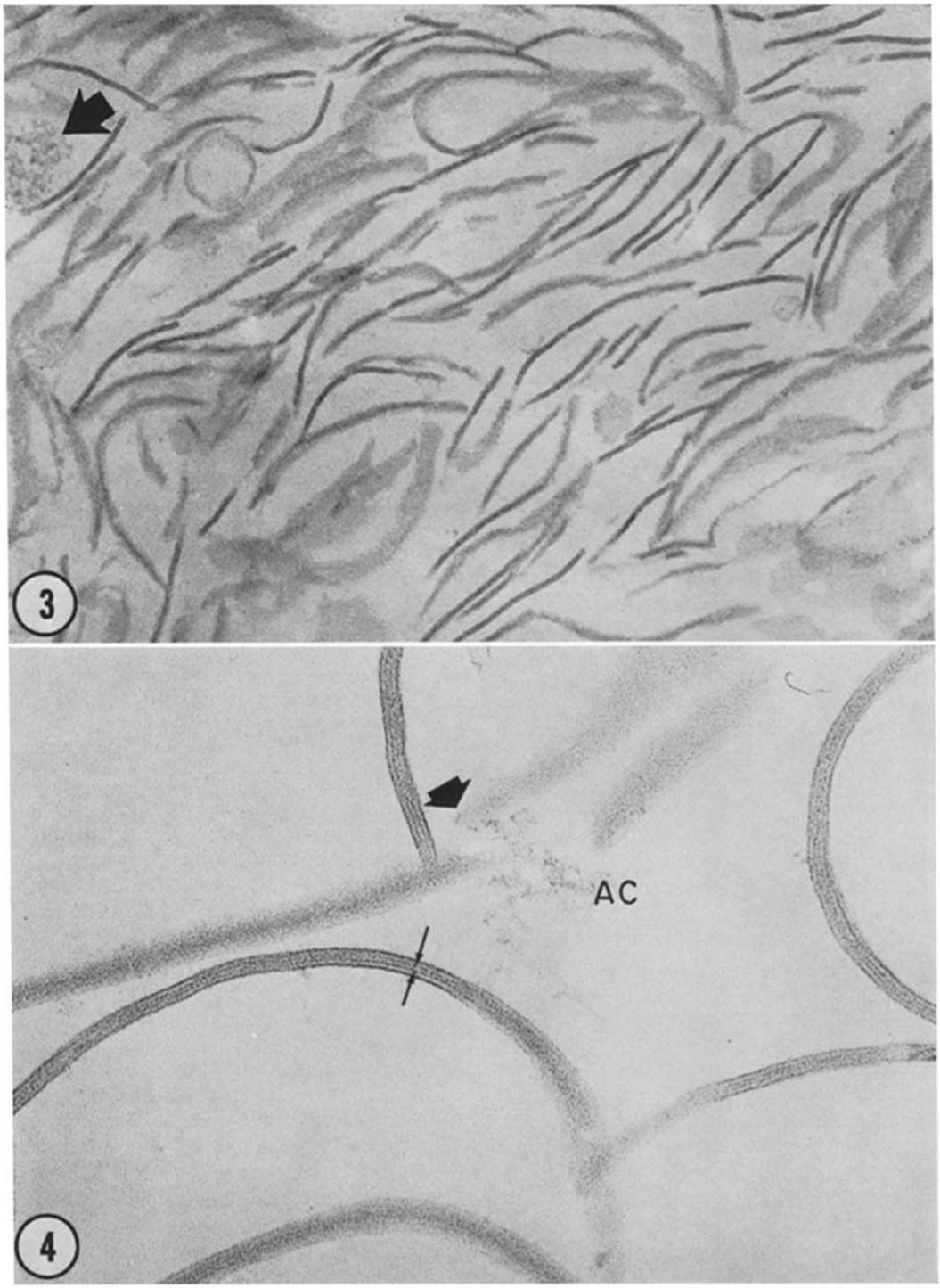

FIGURE 3 A thin section of the pellet obtained from the isolation procedure at low magnification. The pellet contains mostly gap junctions, although some amorphous contamination is visible (arrow). × 61,400.

FIGURE 4 The pellet of isolated gap junctions at high magnification. The junctions still have their characteristic 2 nm gaps (small arrows). The amorphous contamination (*AC*) is visible here, and it frequently appears associated with the ends of the junctions (arrow). × 163,000.

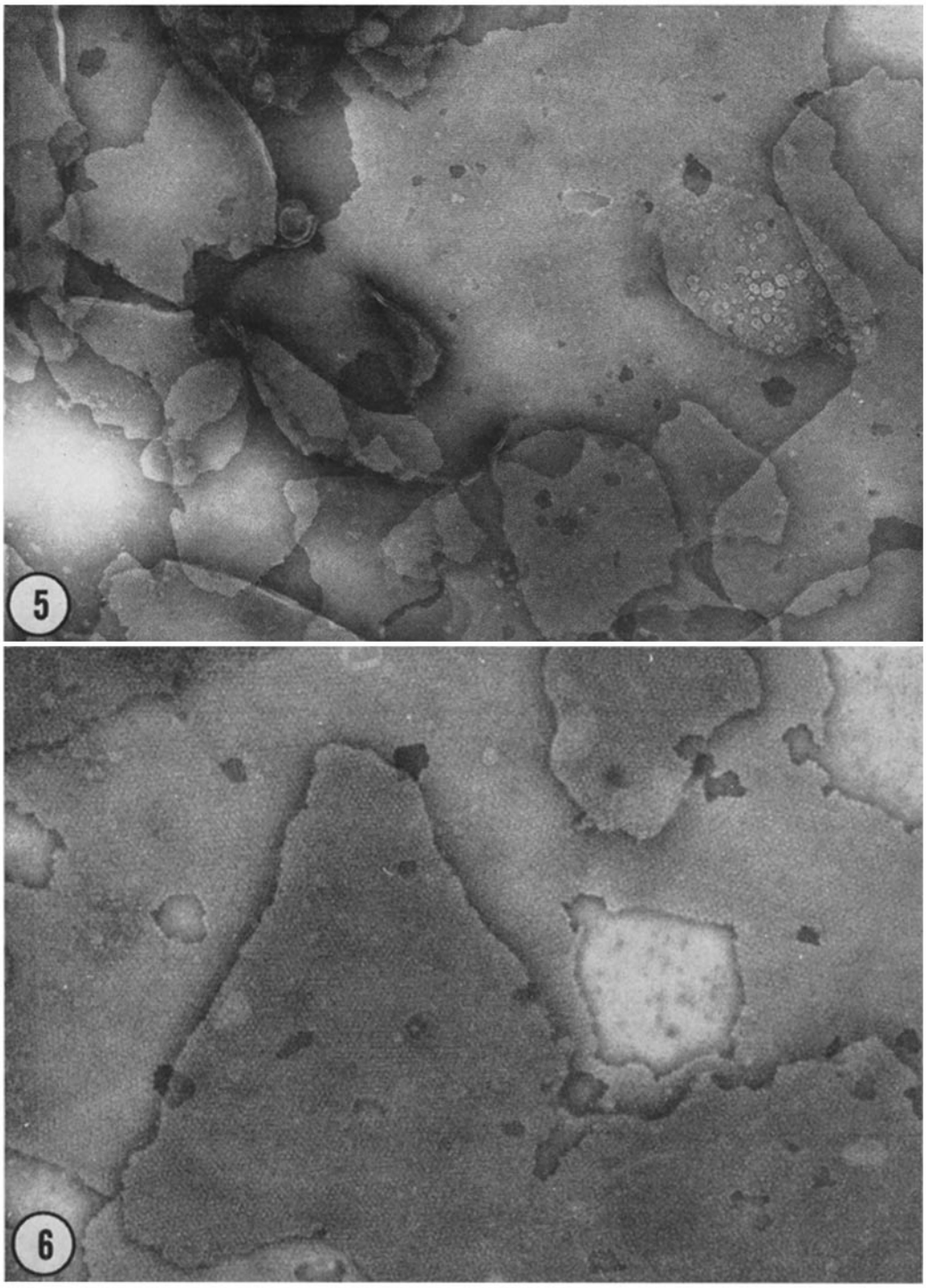

FIGURES 5 and 6 Negatively stained (sodium phosphotungstate) gap junctions from the isolated preparation. The lattice of subunits appears intact and regular following the isolation procedure. Fig. 5, × 81,900; Fig. 6, × 123,300.

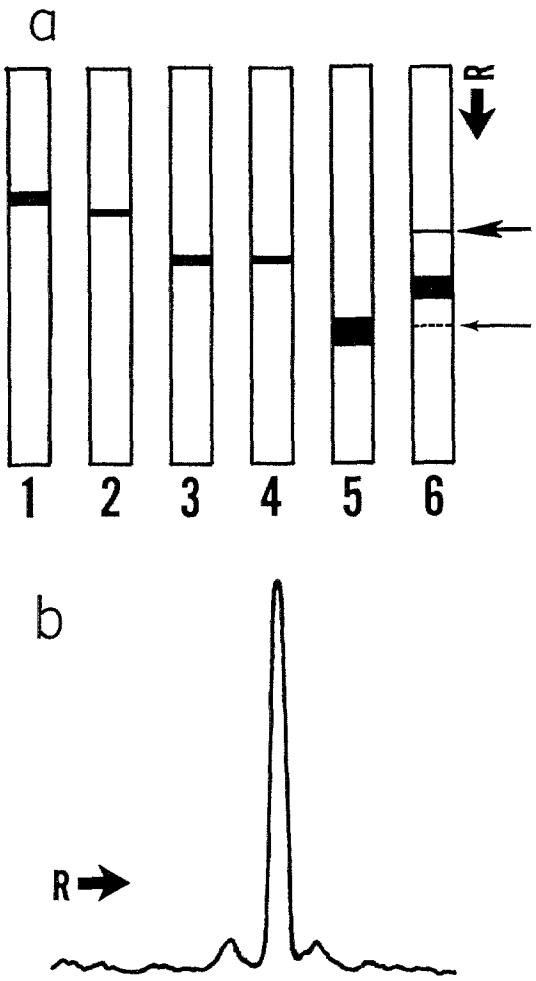

FIGURE 7 Fig. 7 *a* is a drawing of six polyacrylamide gels run with 1% SDS. The first five gels contain marker proteins: 1 = bovine serum albumin, 2 = pepsin, 3 = α-chymotrypsin, 4 = trypsin, 5 = pancreatic RNase. Tube 6 contains the gap junction pellet treated with 1% SDS for 1 hr before running Tube 6 shows one major band, flanked by two minor bands of heavier (large arrow) and lighter (fine arrow) molecular weight. Fig. 7 *b* is a microdensiometric scan of a photograph of tube 6, showing the relative intensities of the three components. The arrows labeled *R* in both (*a*) and (*b*) indicate the direction of electrophoresis.

Figs. 9 and 10 show low-angle X-ray diffraction patterns from isolated junction pellets Spacings were calculated from these films as Bragg reflections Fig 9 is a pattern from a wet pellet of the junction and shows two strong rings at 0 0138 A^{-1} and 0 023 A^{-1}. Fig. 10 is a pattern from the junctional pellet after drying in the capillary tube The meridian shows maxima at 0.0061, 0 0133, 0.02, and 0.0252 A^{-1}. The equatorial reflections show three peaks at 0 0135, 0.0235, and 0 0358–0.04 A^{-1}. Table I shows these results tabulated beside diffraction maxima expected from a lamellar structure 150 A thick with a hexagonal lattice in the plane of the membranes with a center-to-center distance of 86 A.

As can be seen from Table I, the wet junction pattern and the equatorial reflections of the dried junction pattern index closely to the spacings predicted from a hexagonal array of subunits with a center-to-center distance of 86 A. The meridional reflections of Fig. 10, however, index closely to the spacings expected from a lamellar structure of 150 A thickness, and hence may correspond to the junctional profile

At much higher angles, not reproduced in Fig. 10, it is possible to see two broad, diffuse bands at 0.095 and 0 23 A^{-1}, probably arising from protein and lipid, respectively (8).

DISCUSSION

The isolation method described in this paper yields a small quantity (0 1–0.5 mg protein) of relatively pure gap junctions from 36 mouse livers (60 g of tissue). Morphometric data have revealed that 1.5% of the 0.9 m^2/g of membrane surface in mouse liver is occupied by gap junctions (R. Bolender, personal communication). Assuming a density of $d = 1.16$ and a profile thickness of 150 A for the junctions, the yield of gap junctions obtained with this isolation method is in the range of 10%.

The isolated junction preparation contains varying amounts of amorphous contamination visible in thin-sectioned and negatively stained specimens. Because this amorphous material is frequently associated with the edges of the gap junctions, it appears likely that the contaminant arises from residual nonjunctional plasma membranes

Preliminary chemical analyses of the preparation with SDS polyacrylamide gel electrophoresis and thin-layer chromatography reveal that the junctions have a relatively simple protein and lipid composition The electrophoresis gels show one major protein peak with an apparent mol wt of 20,000. It has not been determined at this time whether the two minor peaks are junctional proteins or whether they are related to the amorphous contamination. The lipid composition of the junc-

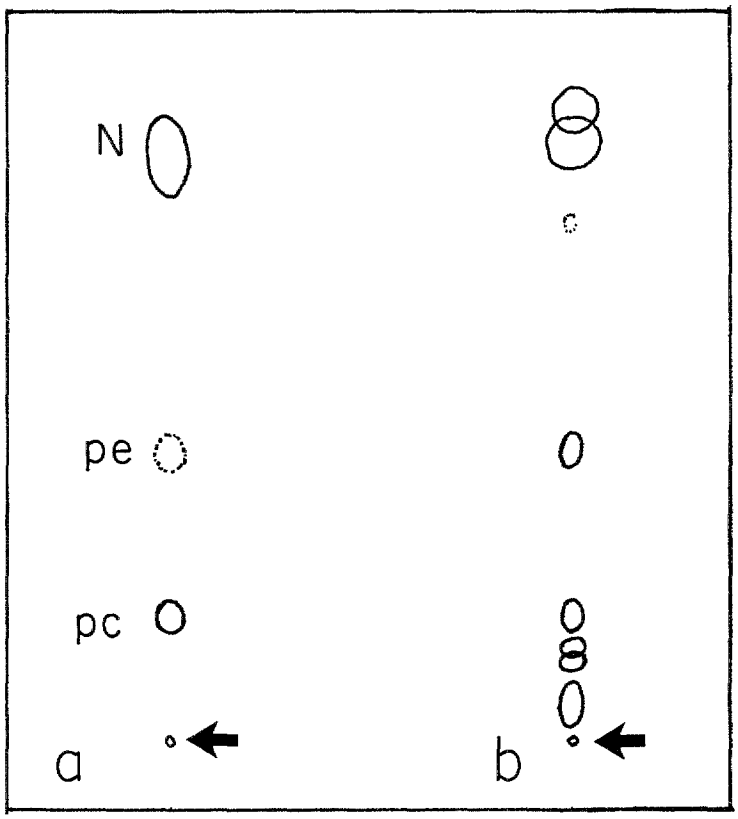

FIGURE 8 A drawing of a thin-layer chromatogram. Fig. 8 *a* is a chloroform-methanol extract of the isolated gap junction preparation, and, for comparison, Fig. 8 *b* is an extract of the crude whole membrane pellet. The origins of both samples are indicated by the arrows. The gap junctions (*a*) show a strong spot tentatively identified as phosphatidylcholine (*pc*) and a very weak spot, drawn with dashed lines, with an R_f similar to that of phosphatidylethanolamine (*pe*). Neutral lipid (*N*) may be seen at the solvent front.

tions is also relatively simple when compared to acetone extracts of crude membrane fractions (15), lack of sphingomyelin is noteworthy

X-ray diffraction analysis of the gap junction structure is limited thus far to measurements and indexing of the diffraction maxima; the two maxima from wet pellets at 0 0138 and 0 023 A^{-1} can be indexed as the first two orders of diffraction from an 86 A center-to-center hexagonal lattice. These two maxima are present on the equator in the dried preparations and show little distortion due to drying. An additional equatorial broad band may be detected in the dried pattern in the range of 0 0358 to 0.04 A^{-1} which spans the expected location of the fourth and fifth order reflections The third order reflection, expected at 0 027 A^{-1}, has not been seen on the films thus far The absence of intervening reflections has been known to occur in other systems (5) and has provided significant structural information The 86 A center-to-center lattice seen with X-ray diffraction agrees well with the published electron microscope data (2, 15, 33, 34)

The meridional maxima seen in the dried junctions index closely to a lamellar structure, $h/150$ A, where h is the diffraction order. These results also agree closely with the thickness of the gap junction measured in thin sections (15).

In the wet diffraction patterns (Fig 9), one would also expect a contribution from the continuous diffraction of the junctional profiles (39) One could assume, for simplicity, that the junction profile electron density distribution is dominated by two bilayers separated by a 30 A peak-to-peak "gap " Following this assumption, one could then calculate the square of the Fourier transform of

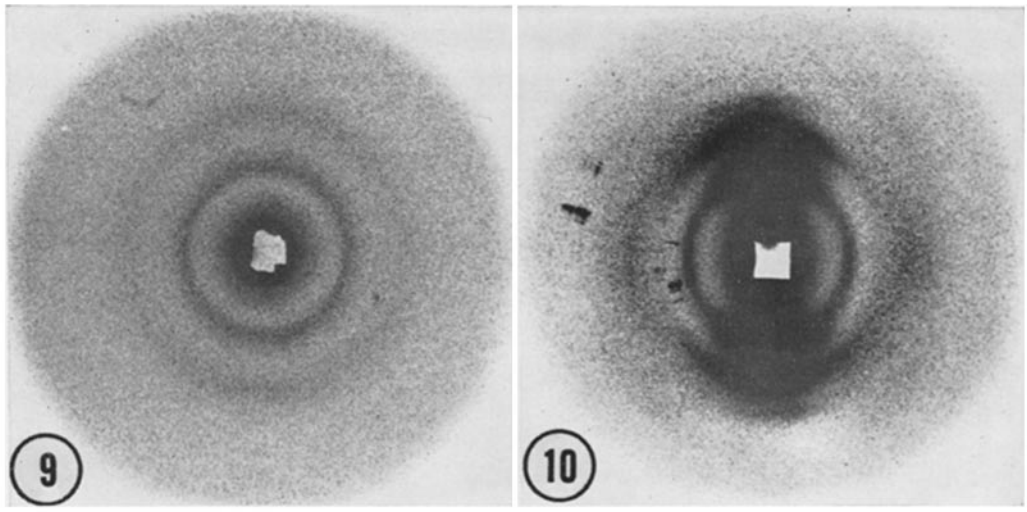

FIGURE 9 An X-ray diffraction pattern from a pellet of wet gap junctions. As summarized in Table I, the two rings index on an 86 A center-to-center hexagonal lattice.

FIGURE 10 An X-ray diffraction pattern from dried gap junctions. The equator shows the same hexagonal reflections seen in Fig. 9, with an additional faint reflection spanning the expected location of the fourth and fifth orders The meridian shows four reflections which fall on the positions expected from a lamellar structure, 150 A thick. The sharp reflections on the left of the pattern are due to scatter from one of the knife edges in the edge of the X-ray beam.

TABLE I

Diffraction Maxima in Reciprocal Space (A^{-1}) Measured from Figs. 9 and 10 Compared to Calculated Maxima

Diffraction order (h)	Measured Fig 9	Measured Fig. 10 equatorial	Calculated hexagonal*	Measured Fig. 10 meridional	Calculated lamellar‡
1	0.0138	0.0135	0 0135	0.0061	0.0067
2	0.023	0.0235	0.0234	0.0133	0.0133
3	—	—	0.027	0.02	0.02
4	—	—	0.0357	0.0252	0.0267
		0.0358–0.04			
5	—		0.405	—	—

* Maxima expected from a hexagonal lattice with a center-to-center spacing of 86 A.
‡ Maxima expected from lamellar sheets 150 A in thickness.

such a density distribution and estimate the location of the expected diffraction maxima (39) Calculations of this sort reveal that the first three maxima would appear at the origin, at 0.0134 A^{-1} and at 0 02 A^{-1}, falling indistinguishably close to the calculated hexagonal reflections and the measured wet reflections summarized in Table I One must conclude, then, that the two rings seen in the wet diffraction patterns may contain contributions from both the 86 A hexagonal lattice and the continuous diffraction from the junctional profiles Additional experiments must be designed to distinguish between these two contributions in the wet preparations.

Apparently, then, the gap junction is a chemically simple membrane fragment, an observation consistent with the regular structure observed in the electron microscope and by X-ray diffraction A similarly simple and highly ordered cell membrane fragment has been isolated recently from a bacterium (4, 29). This chemical simplicity should not be unexpected since isolated differentiated

sites should show a composition with fewer components than the highly complex patterns found in complete cell membranes In the case of the gap junctions the regular structure of the membrane domains should greatly facilitate a complete structural analysis of the molecular level, essential for an understanding of the detailed mechanisms of physiological function. While the gap junction membrane domains are highly specialized, they may nevertheless show some fundamental principles of membrane structure Of special interest should be a study of how they arise in an undifferentiated membrane

The helpful technical assistance of Mrs. Joanne Ventura is gratefully appreciated We would like to thank Drs D. L. D Caspar, G T. King, V. K. Miyamoto, and W Wober for their advice, support, and friendship. We are grateful to Dr. R. Bolender for access to unpublished data.

This work was supported in part by National Science Foundation Postdoctoral Fellowship 40017 and Grant HE 06285 from the National Heart and Lung Institute.

Received for publication 13 March 1972, and in revised form 15 May 1972.

BIBLIOGRAPHY

1. ASADA, Y , and M V. L BENNET. 1971. Experimental alteration of coupling resistance at an electrotonic synapse. *J. Cell Biol.* **49**:159.
2. BENEDETTI, E. L , and P EMMELOT. 1965. Electron microscope observations on negatively stained plasma membranes isolated from rat liver. *J Cell Biol.* **26**:299.
3. BENEDETTI, E. L., and P. EMMELOT 1968. Hexagonal array of subunits in tight junctions separated from isolated rat liver plasma membranes *J Cell Biol.* **38**:15.
4. BLAUROCK, A. E., and W STOECKENIUS. 1971. Structure of the purple membrane *Nat. New Biol.* **233**:152.
5. CASPAR, D. L. D., and D. A. KIRSCHNER. 1971. Myelin membrane structure at 10*A* resolution. *Nat. New Biol* **231**:46.
6. CHALCROFT, J. P , and S BULLIVANT. 1970. An interpretation of liver cell membrane and junction structure based on observation of freeze-fracture replicas of both sides of the fracture. *J. Cell Biol* **47**:49.
7. DEWEY, M. M., and L. BARR. 1962. Intercellular connections between smooth muscle cells: the nexus. *Science (Wash D C)*. **137**:670.
8. ENGELMAN, D. M. 1970. X-ray diffraction studies phase transitions in the membrane of *Mycoplasma laidlawii J. Mol. Biol* **47**:115
9. FLOWER, N. E 1971 Septate and gap junctions between the epithelial cells of an invertebrate, the mollusc *Comnella muculosa J Ultrastruct. Res.* **37**:259.
10. FRANKS, A. 1955 An optically focussing X-ray diffraction camera. *Proc Phys Soc. Lond. Sect. B* **68**:1054.
11. FURSHPAN, E. J 1964 "Electrical transmission" at an excitatory synapse in a vertebrate brain *Science (Wash. D C.)* **144**:878.
12. FURSHPAN, E. J , and D. D POTTER. 1968 Low resistance junctions between cells in embryos and tissue culture. *Curr. Top Dev Biol.* **3**:95
13 GILULA, N B., O R. REEVES, and A. STEINBACH 1972 Metabolic coupling, ionic coupling, and cell contacts *Nature (Lond.)*. **235**:262.
14 GILULA, N. B and P. SATIR. 1971. Septate and gap junctions in molluscan gill epithelium *J. Cell Biol.* **51**:869
15 GOODENOUGH, D A , and J P REVEL 1970. A fine structural analysis of intercellular junctions in the mouse liver *J Cell Biol* **45**:272.
16. GOODENOUGH, D. A., and J P. REVEL. 1971. The permeability of isolated and *in situ* mouse hepatic gap junctions studied with enzymatic tracers. *J. Cell Biol.* **50**:81.
17. GOODENOUGH, D A., and W. STOECKENIUS. 1971. Isolation of gap junctions from mouse liver. 11th Annual Meeting of the American Society for Cell Biology 107. (Abstr).
18 GOSHIMA, K. 1970 Formation of nexuses and electrotonic transmission between myocardial and FL cells in monolyer culture. *Exp Cell Res* **63**:124.
19. HAGOPIAN, M. 1970. Intercellular attachments of cockroach nymph epidermal cells. *J. Ultrastruct Res.* **33**: 233.
20. HAND, A. R., and S. GOEL. 1972. The structural organization of the septate and gap junctions in *Hydra. J. Cell Biol.* **52**:397.
21. HUDSPETH, A J., and J. P. REVEL. 1971. Coexistance of gap and septate junctions in an invertebrate epithelium. *J. Cell Biol* **50**:92.
22 HYDE, A , B. BLONDEL, A. MATTER, J. P. CHENEVAL, B. FILLOUX, and L. GIRARDIER. 1969. Homo- and heterocellular junctions in cell cultures· an electrophysiological and morphological study. *Prog. Brain Res* **31**:283.
23 KREUTZIGER, G. O. 1968. Freeze-etching of intercellular junctions of mouse liver. Proceedings of the Electron Microscope Society of America. **26**:234.
24. LOWENSTEIN, W. R. 1970 Intercellular communication. *Sci. Am.* **222**:78.
25. MAURER, H R. 1968. Disk-Elektrophorese. Walter De Gruyter & Co., Berlin.

26. McNUTT, N. S., and R. S. WEINSTEIN. 1970. The ultrastructure of the nexus. A correlated thin-section and freeze-cleave study *J. Cell Biol.* **47**:666.
27. MUIR, A. R. 1967. The effect of divalent cations on the ultrastructure of the perfused rat heart. *J. Anat.* **101**:239.
28. OSCHMAN, J. L., and M. J. BERRIDGE. 1970. Structural and functional aspects of salivary fluid in *Calliphora*. *Tissue Cell.* **2**:281.
29. OSTERHELT, D., and W. STOECKENIUS. 1971. Rhodopsin-like protein from the purple membrane of *Halobacterum halobium*. *Nat. New Biol.* **233**:149.
30. PAPPAS, G. D., Y. ASADA, and M. V. L BENNETT. 1971. Morphological correlates of increased coupling resistance at an electrotonic synapse. *J. Cell Biol.* **49**:173.
31. PAPPAS, G. D., and M. V. L. BENNETT. 1966. Specialized junctions involved in electrical transmission between neurons. *Ann. N. Y. Acad. Sci.* **137**:495.
32. PAYTON, B W., M. V. L. BENNET, and G. D. PAPPAS. 1969. Permeability and structure of junctional membranes at an electrotonic synapse. *Science* (*Wash. D C.*) **166**:1641.
33. REVEL, J. P., and M. J. KARNOVSKY. 1967. Hexagonal array of subunits in intercellular junctions of the mouse heart and liver. *J. Cell Biol.* **33**:C7.
34. ROBERTSON, J. D. 1963. The occurrence of a subunit pattern in the unit membranes of club endings in Mauthner cell synapses in goldfish brains. *J. Cell Biol.* **19**:201.
35. ROSE, B. 1971. Intercellular communication and some structural aspects of membrane junctions in a simple cell system. *J. Membrane Biol.* **5**:1.
36 SEGREST, J. P., R. L. JACKSON, E. P. ANDREWS, and V. T. MARCHESI. 1971. Human erythrocyte membrane glycoprotein: a reevaluation of the molecular weight as determined by SDS polyacrylamide gel electrophoresis. *Biochem. Biophys. Res. Commun.* **44**:390.
37. STOECKENIUS, W., and D. M. ENGELMAN. 1969. Current models for the structure of biological membranes. *J. Cell Biol.* **42**:613.
38. WAGNER, H., L. HORHAMMER, and P. WOLFF. 1961. Dunnschichtochromatographie von Phosphatiden und Glykolipiden. *Biochem. Z.* **334**:175.
39. WILKINS, M. H. F., A. E. BLAUROCK, and D. M. ENGLEMAN. 1971. Bilayer structure in membranes. *Nat. New Biol.* **230**:72.
40. ZAMPIGHI, G., and J. D. ROBERTSON. 1971. An electron microscopic study of subunit structure in synaptic disks of goldfish medulla oblongata. Proceedings of the 11th Annual Meeting of the American Society for Cell Biology. 336. (Abstr.)
41. ZAMPIGHI, G., and J. D. ROBERTSON. 1972. Fine structure of synaptic disks of goldfish medulla. *Anat. Rec.* **172**:434.